g14 beam-target helicity asymmetries for $\vec{\gamma}\vec{n} \to \pi^- p$

PHYSICAL REVIEW LETTERS

Beam-Target Helicity Asymmetry for $\vec{\gamma}\vec{n} \to \pi^- p$ in the N^* Resonance Region

D. Ho,[2] P. Peng,[16] C. Bass,[1] P. Collins,[3] A. D'Angelo,[1,15] A. Deur,[1] J. Fleming,[4] C. Hanretty,[1,16] T. Kageya,[1] M. Khandaker,[8] F. J. Klein,[5,*] E. Klempt,[7] V. Laine,[12] M. M. Lowry,[1] H. Lu,[2,14] C. Nepali,[9] V. A. Nikonov,[7,10] T. O'Connell,[13] A. M. Sandorfi,[1,*] A. V. Sarantsev,[7,10] R. A. Schumacher,[2] I. I. Strakovsky,[5] A. Švarc,[11] N. K. Walford,[3] X. Wei,[1] C. S. Whisnant,[6] R. L. Workman,[5] I. Zonta,[15] K. P. Adhikari,[35,9] D. Adikaram,[9] Z. Akbar,[25] M. J. Amaryan,[9] S. Anefalos Pereira,[27] H. Avakian,[1] J. Ball,[33] M. Bashkanov,[4] M. Battaglieri,[28] V. Batourine,[1] I. Bedlinskiy,[32] A. Biselli,[23] W. J. Briscoe,[5] V. D. Burkert,[1] D. S. Carman,[1] A. Celentano,[28] G. Charles,[9,33] T. Chetry,[36] G. Ciullo,[26] L. Clark,[39] L. Colaneri,[13] P. L. Cole,[30] M. Contalbrigo,[26] V. Crede,[25] N. Dashyan,[45] E. De Sanctis,[27] R. De Vita,[28] C. Djalali,[42] R. Dupre,[31,33] A. El Alaoui,[43,17] L. El Fassi,[35,17] L. Elouadrhiri,[1] P. Eugenio,[25] G. Fedotov,[42,38] S. Fegan,[39] R. Fersch,[21,22] A. Filippi,[29] A. Fradi,[31] Y. Ghandilyan,[45] G. P. Gilfoyle,[41] F. X. Girod,[1] D. I. Glazier,[39,4] C. Gleason,[42] W. Gohn,[13] E. Golovatch,[38] R. W. Gothe,[42] K. A. Griffioen,[22] M. Guidal,[31] L. Guo,[24] H. Hakobyan,[43,45] N. Harrison,[1,13] M. Hattawy,[17] K. Hicks,[36] M. Holtrop,[40] S. M. Hughes,[4] Y. Ilieva,[42] D. G. Ireland,[39] B. S. Ishkhanov,[38] E. L. Isupov,[38] D. Jenkins,[44] H. Jiang,[42] H. S. Jo,[31] K. Joo,[13] S. Joosten,[37] D. Keller,[16] G. Khachatryan,[45] A. Kim,[13,34] W. Kim,[34] A. Klein,[9] V. Kubarovsky,[1] S. V. Kuleshov,[43,32] L. Lanza,[15] P. Lenisa,[26] K. Livingston,[39] I. J. D. MacGregor,[39] N. Markov,[13] B. McKinnon,[39] T. Mineeva,[43,13] V. Mokeev,[1] R. A. Montgomery,[39] A. Movsisyan,[26] C. Munoz Camacho,[31] G. Murdoch,[39] S. Niccolai,[31] G. Niculescu,[6] M. Osipenko,[28] M. Paolone,[37,42] R. Paremuzyan,[40,45] K. Park,[1] E. Pasyuk,[1] W. Phelps,[24] O. Pogorelko,[32] J. W. Price,[19] S. Procureur,[33] D. Protopopescu,[39] M. Ripani,[28] D. Riser,[13] B. G. Ritchie,[18] A. Rizzo,[15] G. Rosner,[39] F. Sabatié,[33] C. Salgado,[8] Y. G. Sharabian,[1] Iu. Skorodumina,[38,42] G. D. Smith,[4] D. I. Sober,[3] D. Sokhan,[31,39] N. Sparveris,[37] S. Strauch,[42] Ye Tian,[42] B. Torayev,[9] M. Ungaro,[1] H. Voskanyan,[45] E. Voutier,[31] D. P. Watts,[4] M. H. Wood,[20] N. Zachariou,[4,42] J. Zhang,[1] and Z. W. Zhao[16]

(CLAS Collaboration)

Phys. Rev. Lett. ***118*** *(2017) ; arXiv:1705.04713 [nucl.ex]*

Unfolding and interpreting the N* spectrum

- low energy structure of QCD lies encoded in the excited N* spectrum, a complex overlap of resonances with "dressed" vertices

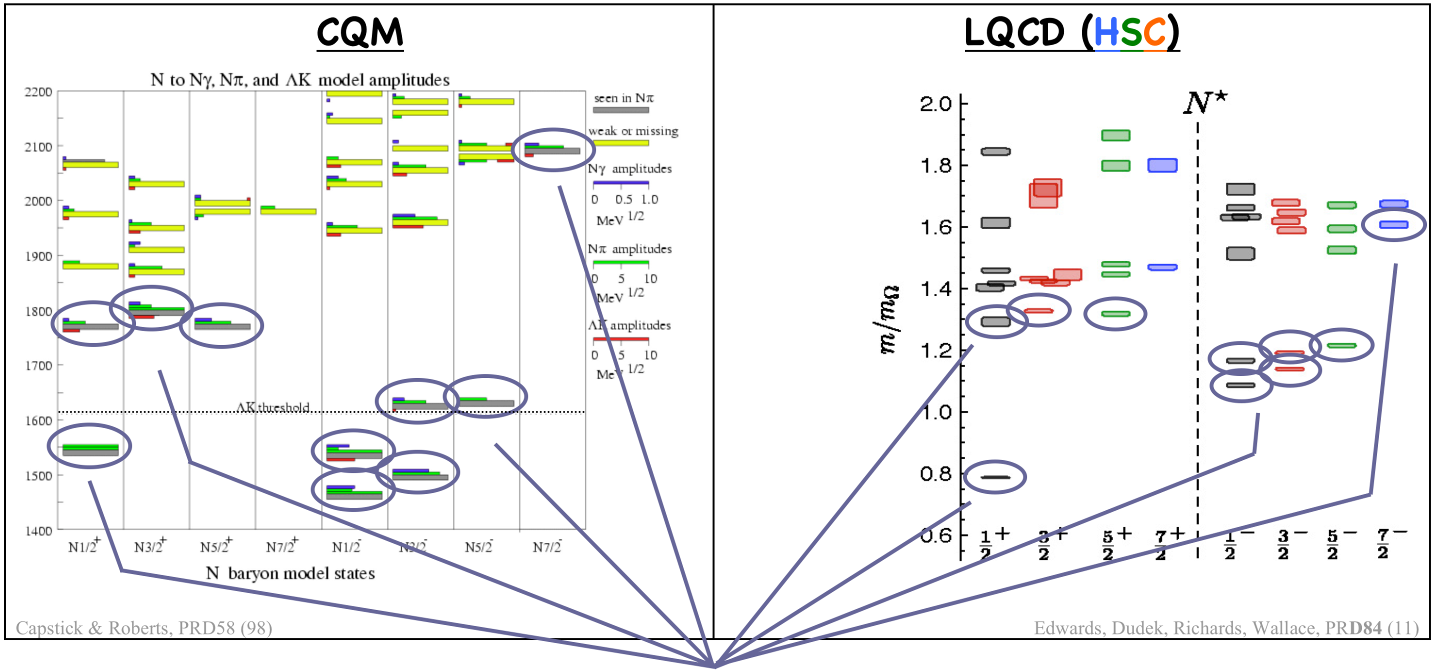

- only lowest few in each band "seen" with 4★ or 3★ PDG status

⇔ need to understand the structure of the states that are observed and find the ones that aren't !

the physics of "dressed" QCD

N resonance ⬄ s-channel pole*

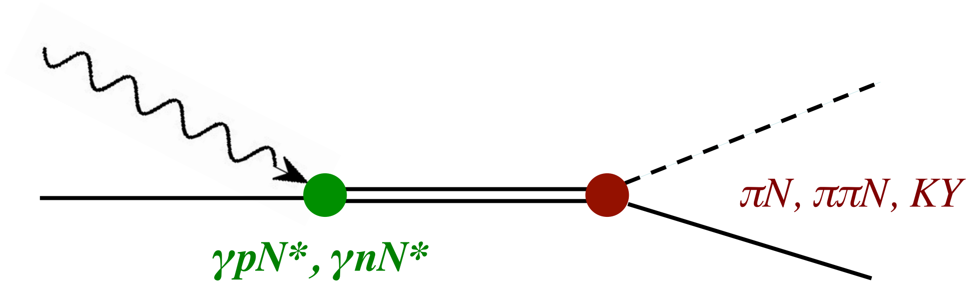

- *meson-loop "dressings" of the Electromagnetic vertex affect the dynamical properties (excitation mechanism) and determine Q^2 evolution, but do not affect the N* spectral properties*

- *coupled-channel "dressings" of the strong vertex determine the N* spectral properties (mass/pole positions, widths)*

- *dressings are beyond the current sophistication of LQCD or DSE field theories*

⬄ models, constrained by the spectrum and its couplings

data needed to unravel the N* spectrum

- $\gamma + N \Rightarrow (J^{\pi}=0^{-}) + N/\Lambda/\Sigma$

spin states: 2 + 2 ⇨ **0 + 2** ⇨ 8 spin combinations
⇨ 4 unique (parity)

⇨ 4 complex amplitudes describe photo-production ⇔ 8 unknows

New goal: (Jlab, Bonn, Mainz)

- measure many polarization observables (of 16) ⇔ lots of proton data

- the electromagnetic interactions do not conserve isospin

$$\mathcal{A}_{\gamma p\to\pi^+ n} = \sqrt{2}\left\{\mathcal{A}_p^{I=1/2} - \tfrac{1}{3}\mathcal{A}^{I=3/2}\right\}$$
$$\mathcal{A}_{\gamma n\to\pi^- p} = \sqrt{2}\left\{\mathcal{A}_n^{I=1/2} - \tfrac{1}{3}\mathcal{A}^{I=3/2}\right\}$$

⇔ *proton data determine* $\mathcal{A}^{I=3/2}$

⇨ *both proton and neutron target data needed for the I= ½ amplitudes*

- *γ+n data base is very sparse*

⇔ *γnN** ***couplings very poorly determined***

E06-101 (g14)

- *Dec'2011 –to- May'2012*
- *tagged photons with circular and linear polarization on polarized HD,*
  E_γ: 700 – 2400 MeV

- *this publication:*
  the beam-target "E" asymmetry in $\gamma D \rightarrow \pi^- p(p)$
  with circularly polarized photons and longitudinally polarized Deuterons,
  W: 1500 – 2300 MeV

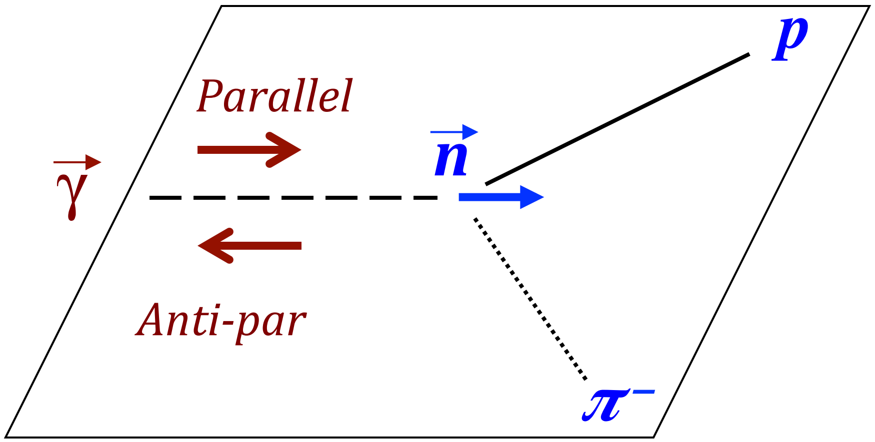

$$E = \frac{1}{P_\gamma P_T} \frac{\sigma_A - \sigma_P}{\sigma_A + \sigma_P}$$

g14 … with the last breath of the CLAS(6) detector

Torus magnet
6 superconducting coils

Electromagnetic calorimeters
Lead/scintillator, 1296 photomultipliers

polarized target + start counter

Drift chambers
argon/CO_2 gas, 35,000 cells

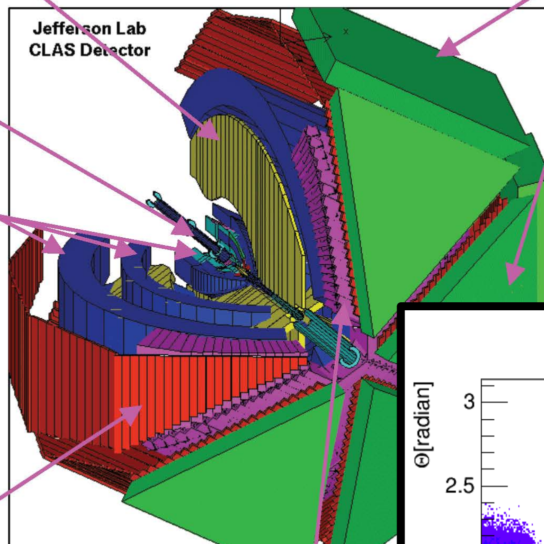

Time-of-flight counters
plastic scintillators, 684 photomultipliers

Gas Cherenkov count
e/π separation, 256 PMT

DAQ linit ~ 6kHz (~1.5TB/day)

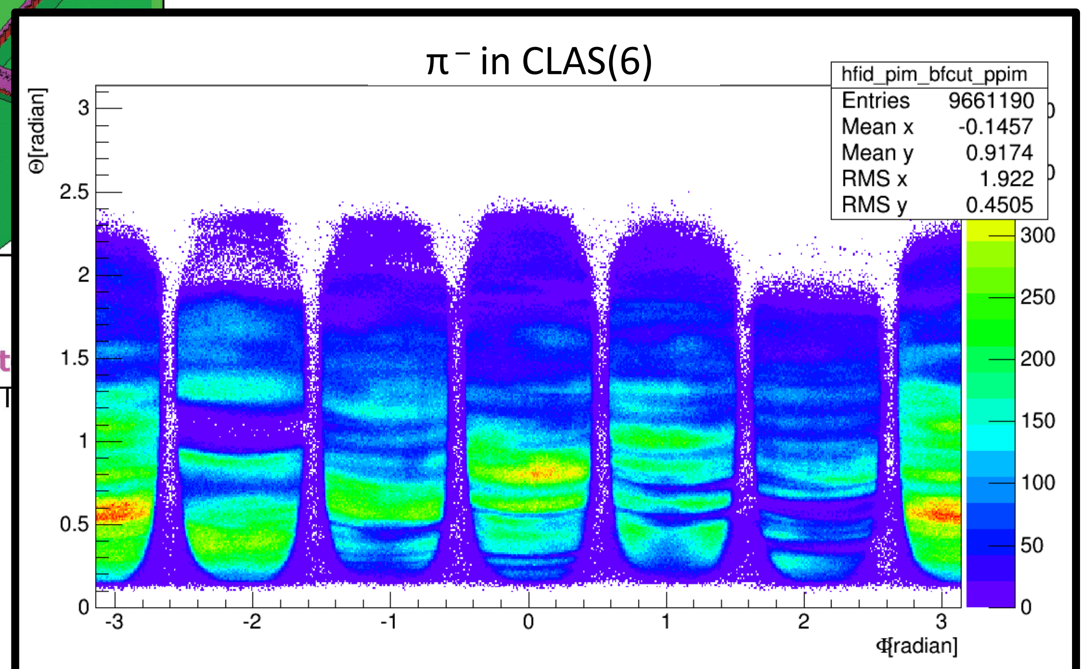

HDice frozen-spin target

- target: $\varnothing$ 15 mm $\times$ 50 mm
- material: solid HD
- dilution factors: 1/1 for $\vec{n}$
  1/2 for $\vec{p}$

- < P(D) > = 25% (ave in g14)
- T_1 (1/e relaxation time) $\sim$ years

- HDice-I: NIM A737 (2014) 107
- HDice-II: NIM A815 (2016) 31

- moved while polarized to Hall B

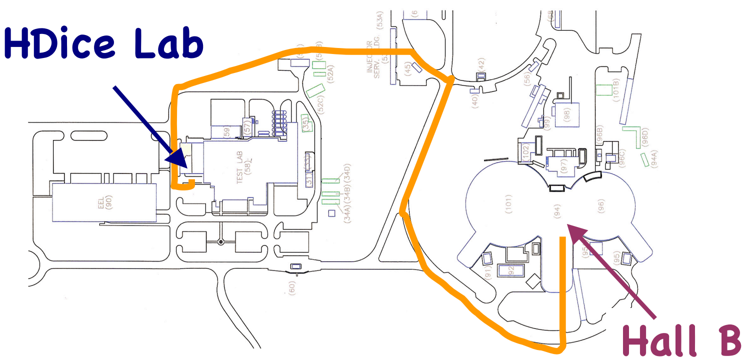

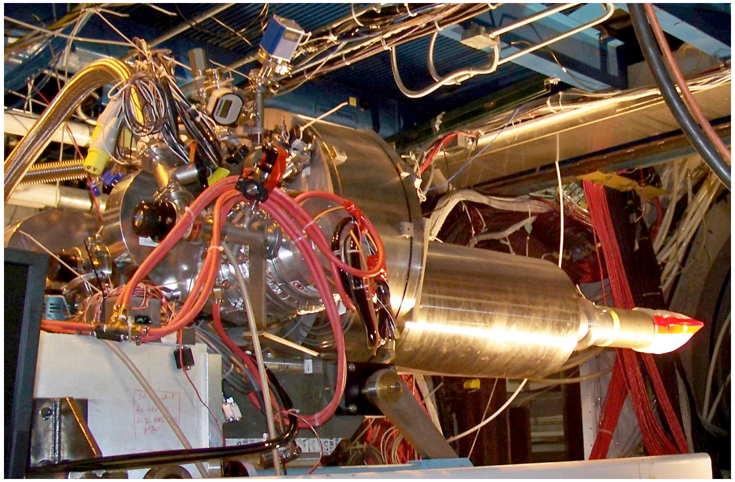

clean deuteron target

- sources of neutrons: D in HD and the target cell
- evaporate and pump away HD: residual backgrounds are small

⇨ after empty cell subtraction, all neutrons are polarizable

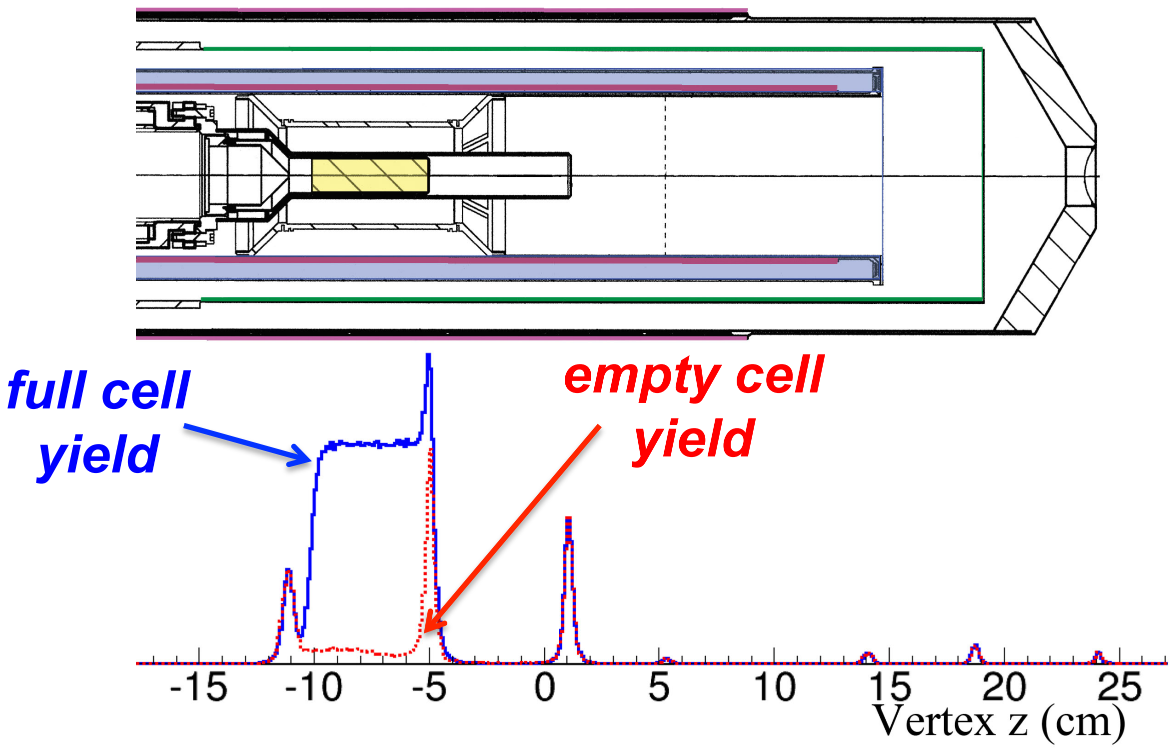

parallel analyses of $\gamma D \rightarrow \pi^- p\ (p)$

- *Bksub* – conventional application of sequential cuts, with **empty subtraction**
- *KinFit* – energy & momentum conservation used in ***Kinematic fitting*** to improve accuracy of measured quantities
- *BDT* – "**Boosted Decision Trees**" used to place *simultaneous* (rather than sequential) requirements
- Vertex preselection:

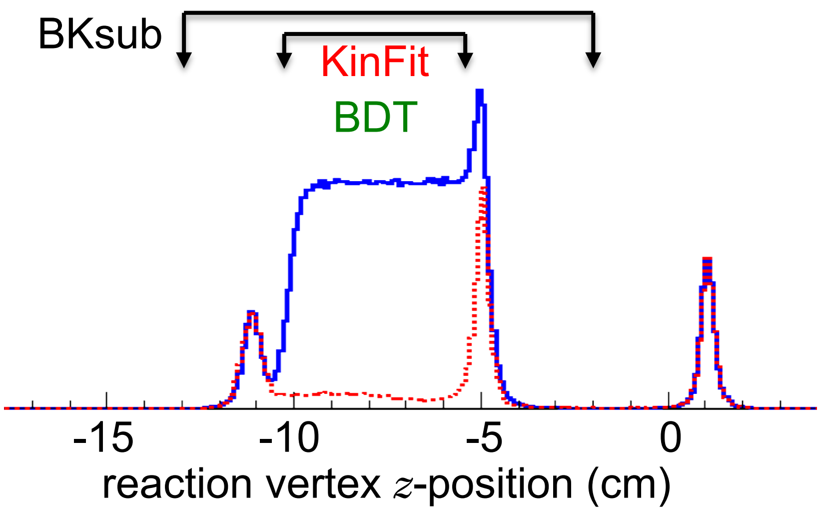

Bksub analysis

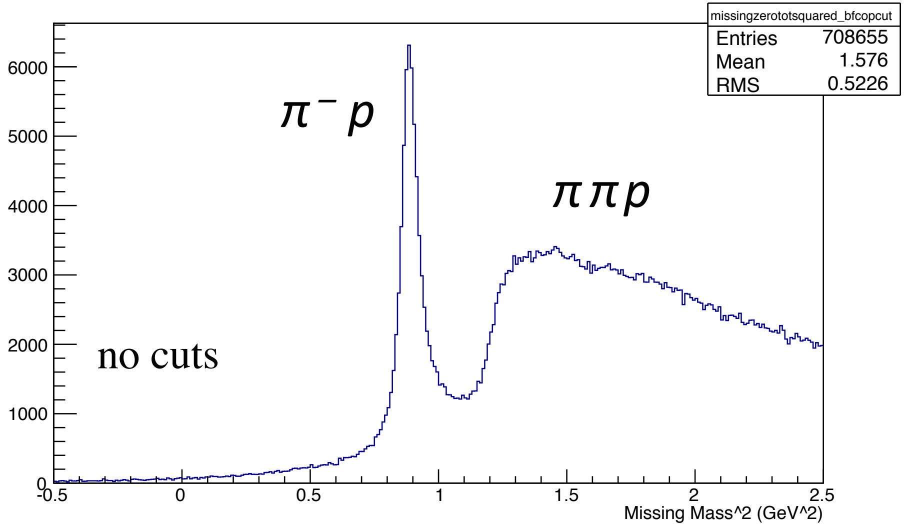

MM^2

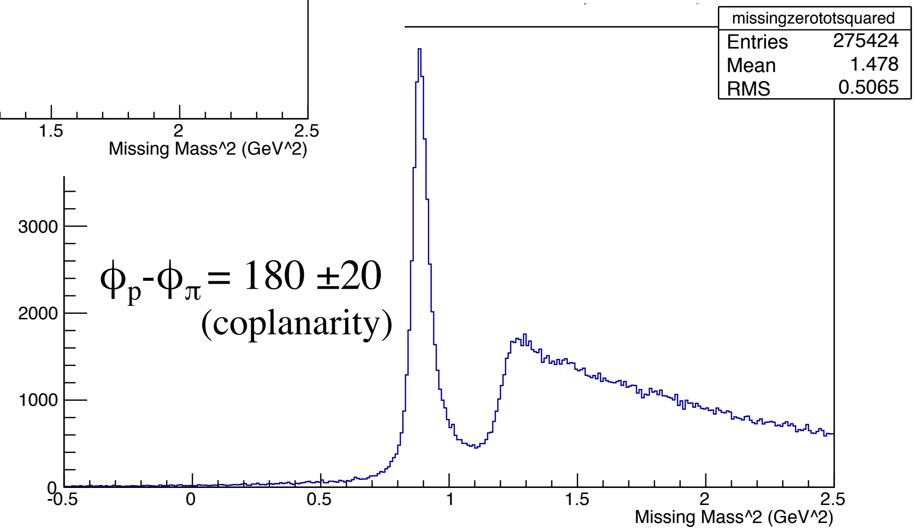

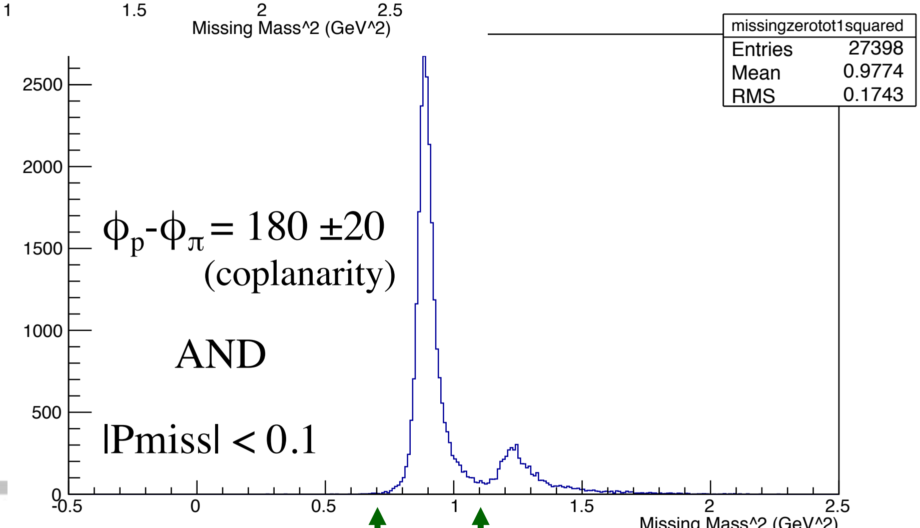

$\gamma D \rightarrow \pi^- p\ (p)$ Missing Mass squared,
with sequential 2-body requirements,
followed by empty cell subtraction

KinFit analysis

- *Kinematic Fitting carried out on candidates for γ+(n) ➔ π^- p*

  ⬄ *target assumed to have the neutron mass, but unknown momentum*

  ⬄ *amounts to a 1C fit*

- *2π & reactions on target cell nucleons fail with Confidence Level < 0.05*
- *accept events with Confidence Level > 0.05*
- apply |P_{miss}| < 0.1 GeV/c to accepted events

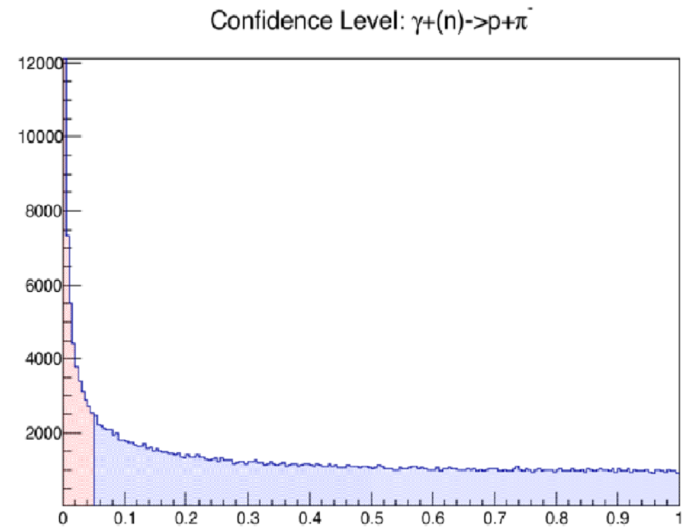

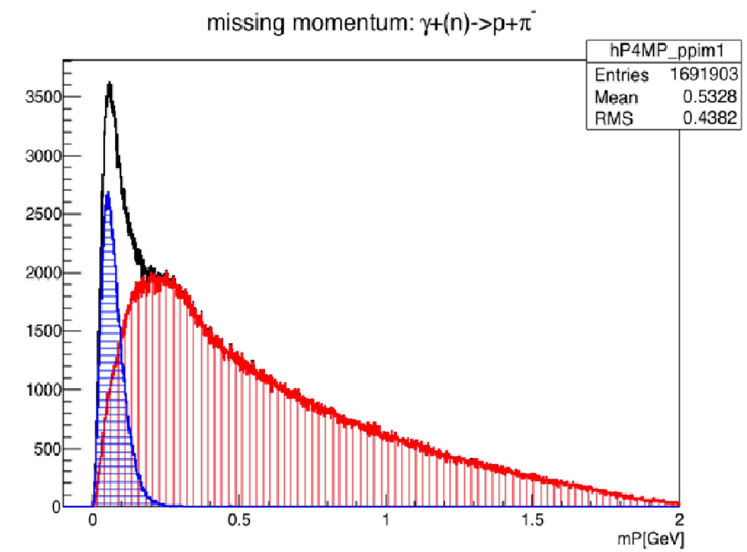

BDT analysis

- multivariate ***Boosted Decision Trees***
  - ⇔ views the data in a higher dimension
  - ⇔ creates a forest of *if-then-else* logical tests on all kinematic variables *simultaneously*
- algorithm categorizes events as either ***signal*** or ***background***
  - *signal trained* on $\gamma D \rightarrow \pi^- p(p)$ from CLAS MC
  - *background trained* on empty-cell data
- apply $|P_{miss}| < 0.1$ GeV/c to *signal* events

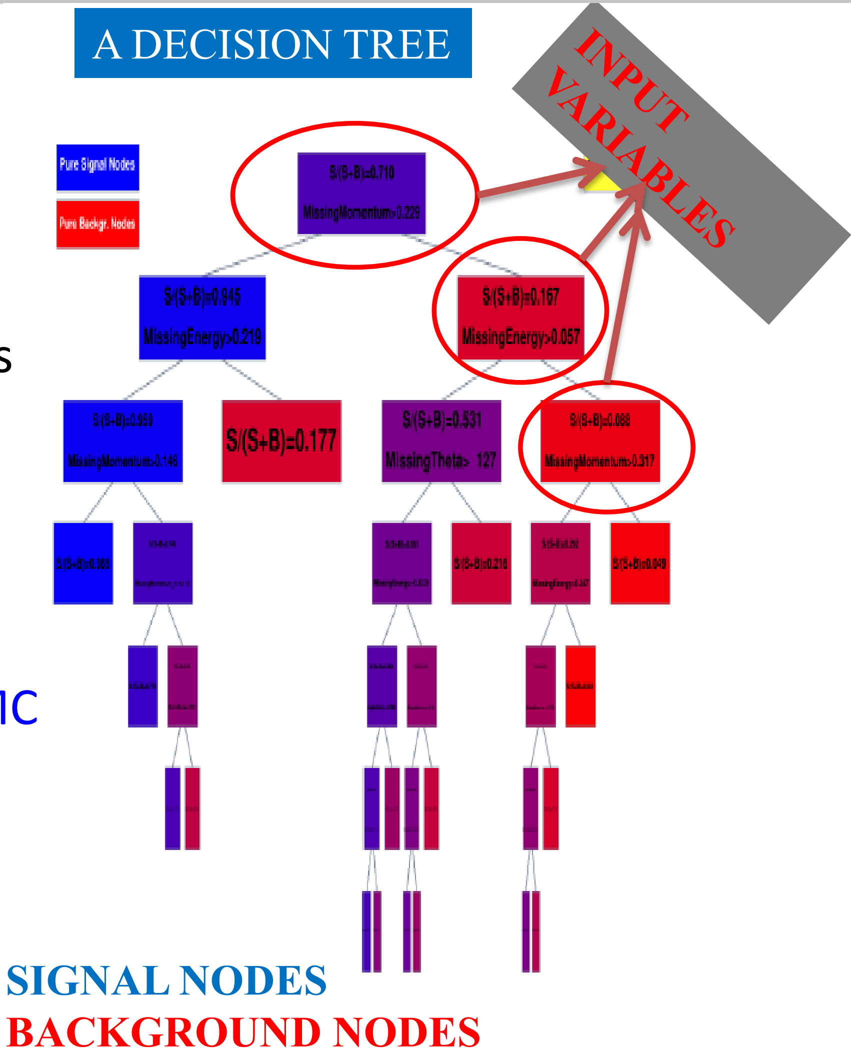

Dao Ho (2015)

Restricting Deuteron reactions to create an effective neutron target

- *select events for which the proton in Deuterium is a passive "spectator"*
  ⇔ *key variable is the momentum of the undetected proton in γ+n(p) ➔ π^- p(p)*

  ⇔ *use the data itself to determine the kinematic region in which the result is stable*

  $|P_{miss}| < 0.1$ GeV/c

  ⇔ *applied in all three analyses*

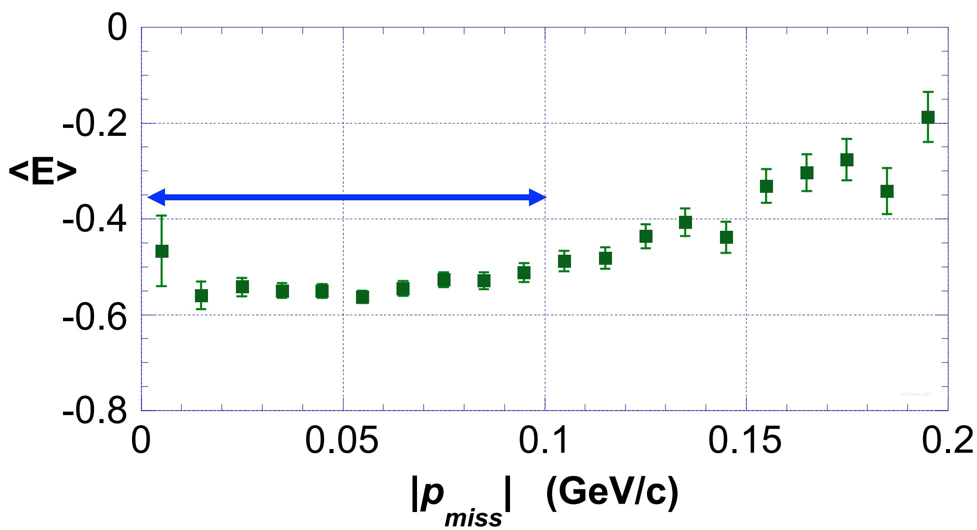

- theory perspective:
  FSI have negligible effect on E asymmetry in π^- *p p final state*
  (I = 1 *pp* final state is orthogonal to the initial deuteron wavefunction)

- effect of deuteron's D-state is negligible after $|P_{miss}| < 0.1$ cut (T.-S. H. Lee)

Combining analyses into the final results

- asymmetries from the three analyses are statistically consistent
- weighted mean is taken as the best estimate of the asymmetry
- correlated errors are fitted to the expected χ^2 { Schmelling, Physica **51** (95)676 }

<u>Advantages</u>

- reduces hidden bias
- acceptance at extreme angles is different for the 3 methods; averaging improves reliability where PWA interference is large

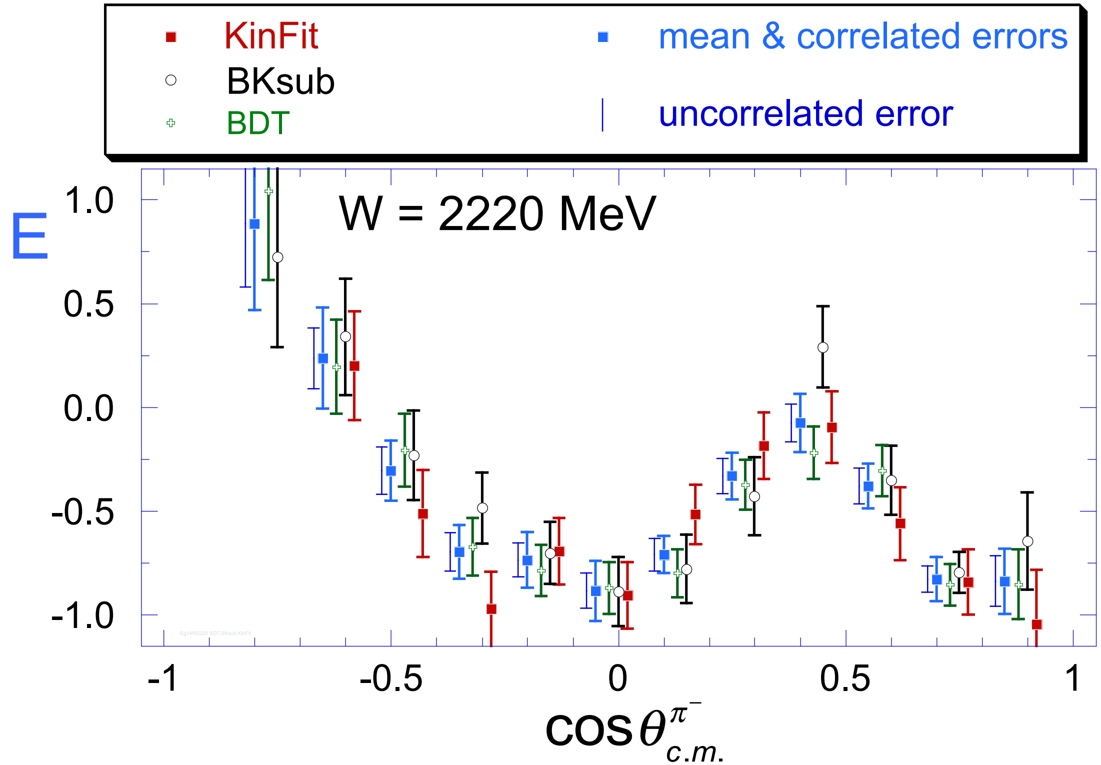

The g14 beam-target "E" asymmetries for $\gamma n \rightarrow \pi^- p$

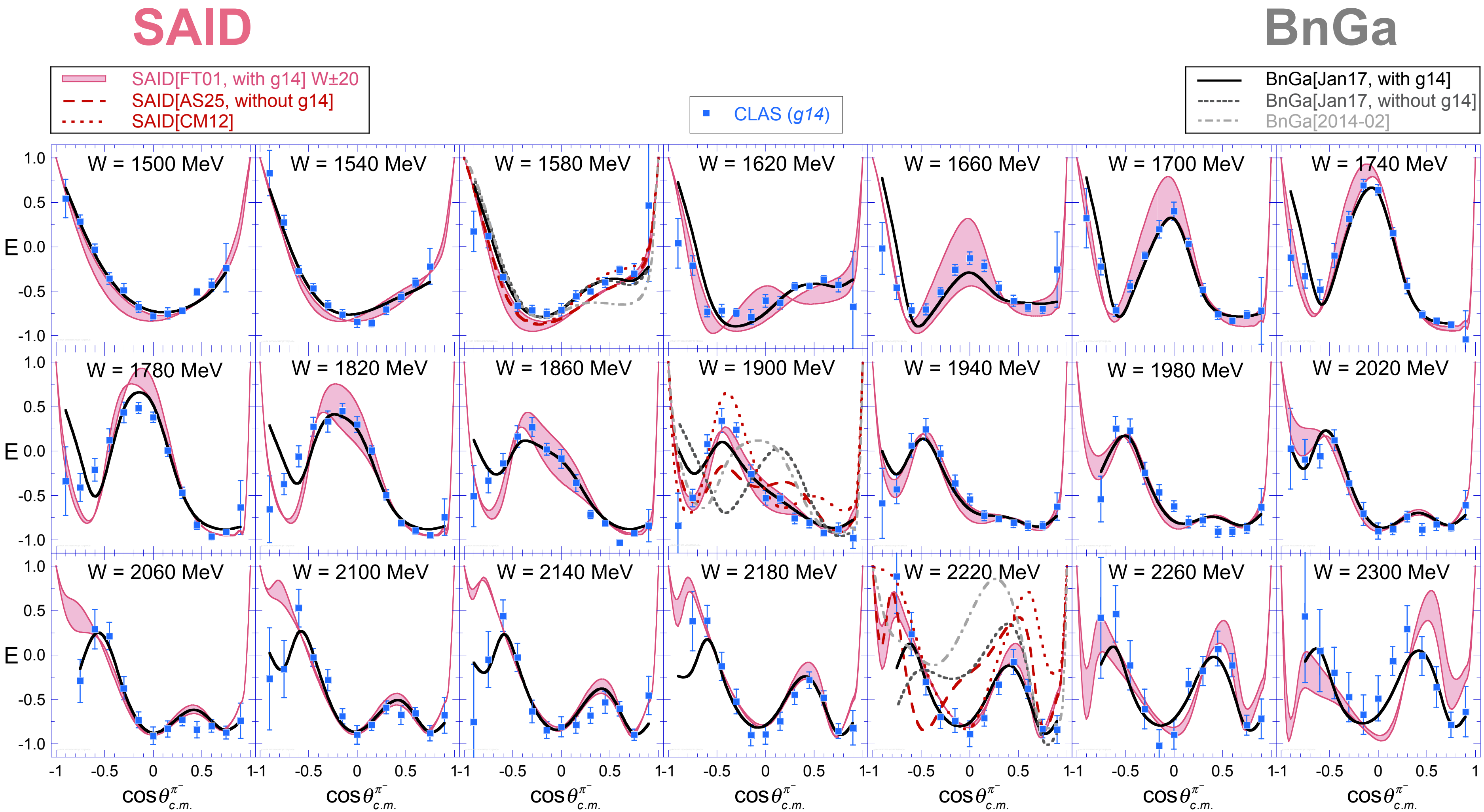

The g14 beam-target "E" asymmetries for $\gamma n \rightarrow \pi^- p$

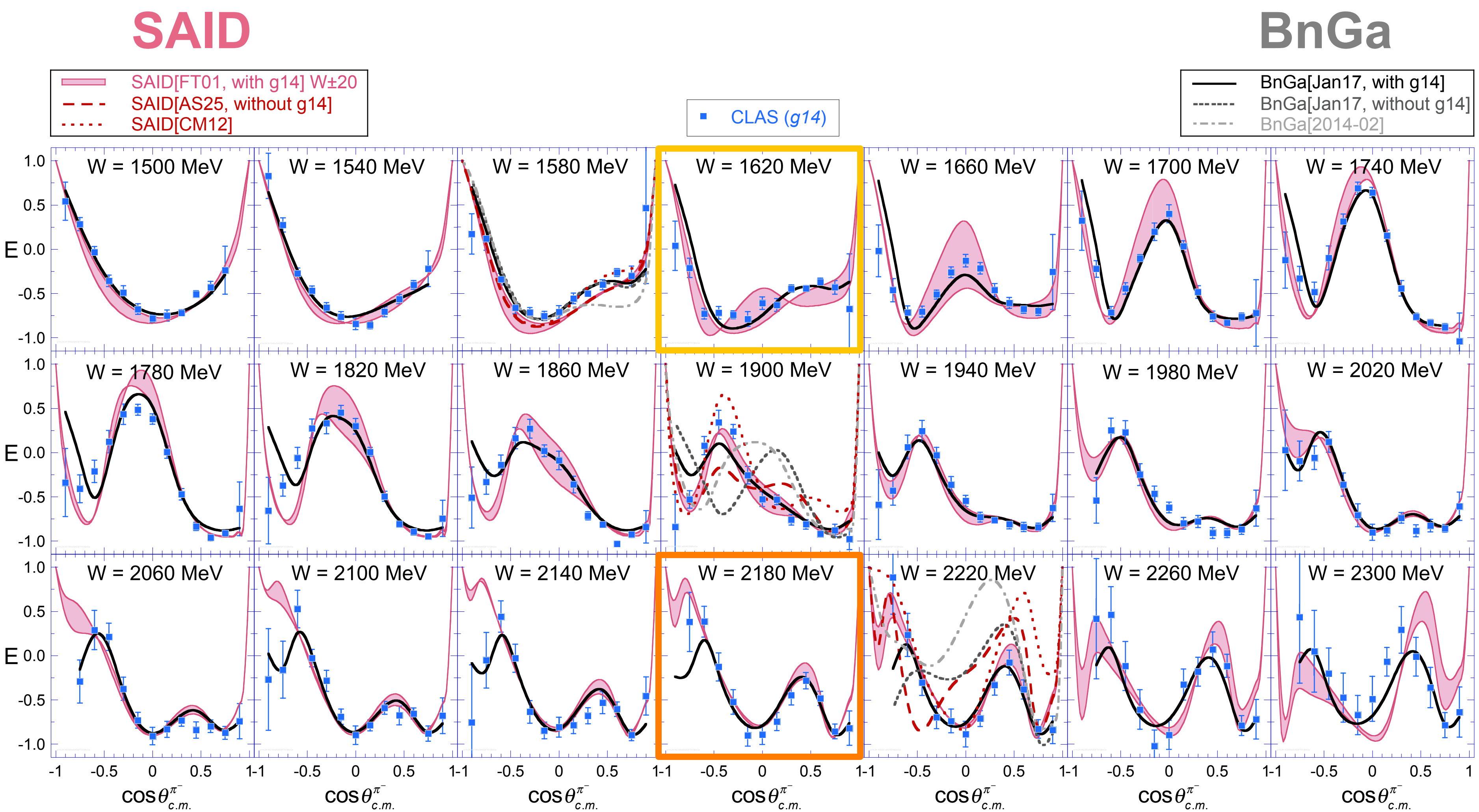

The g14 beam-target "E" asymmetries for $\gamma n \rightarrow \pi^- p$

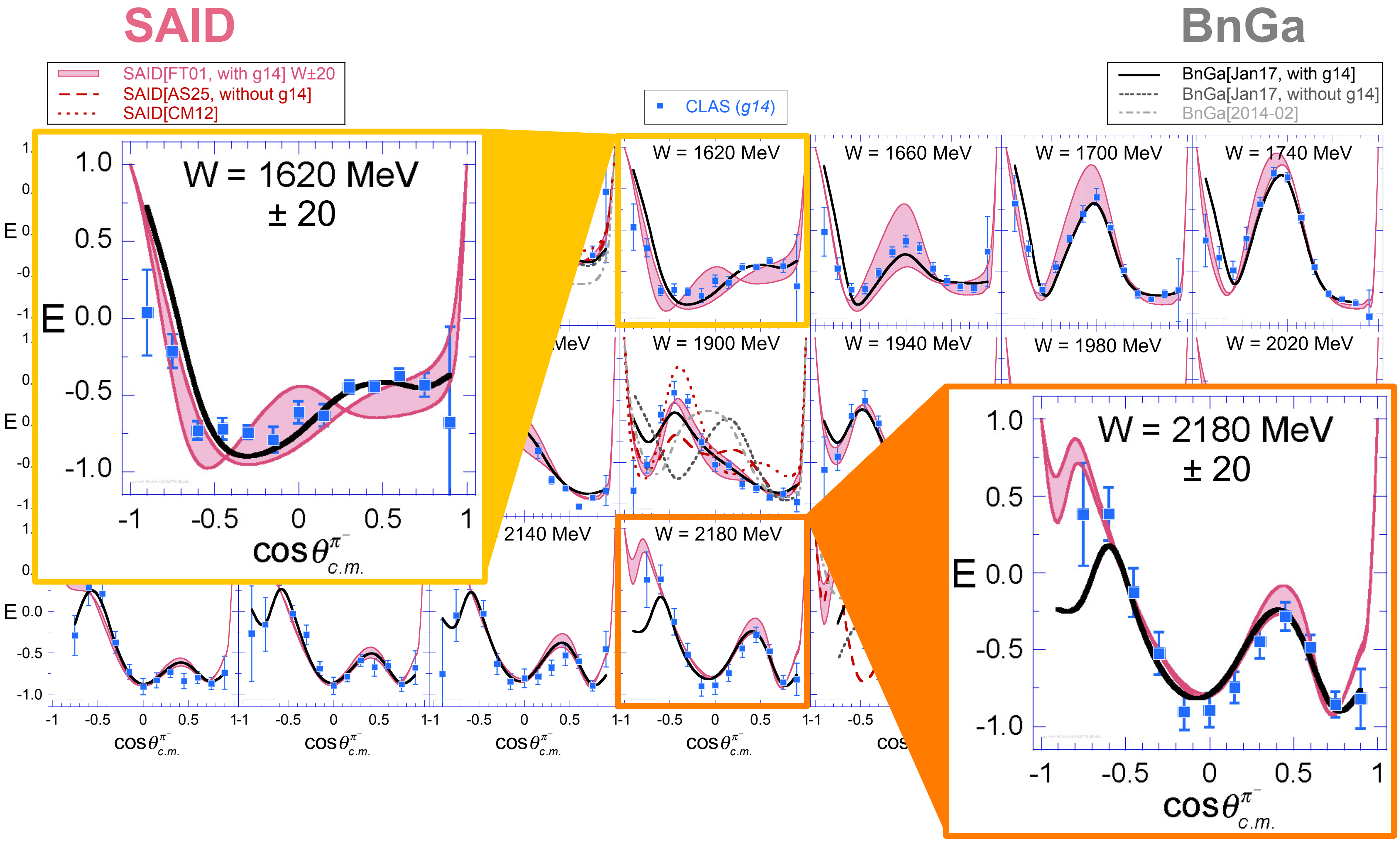

The g14 beam-target "E" asymmetries for $\gamma n \rightarrow \pi^- p$

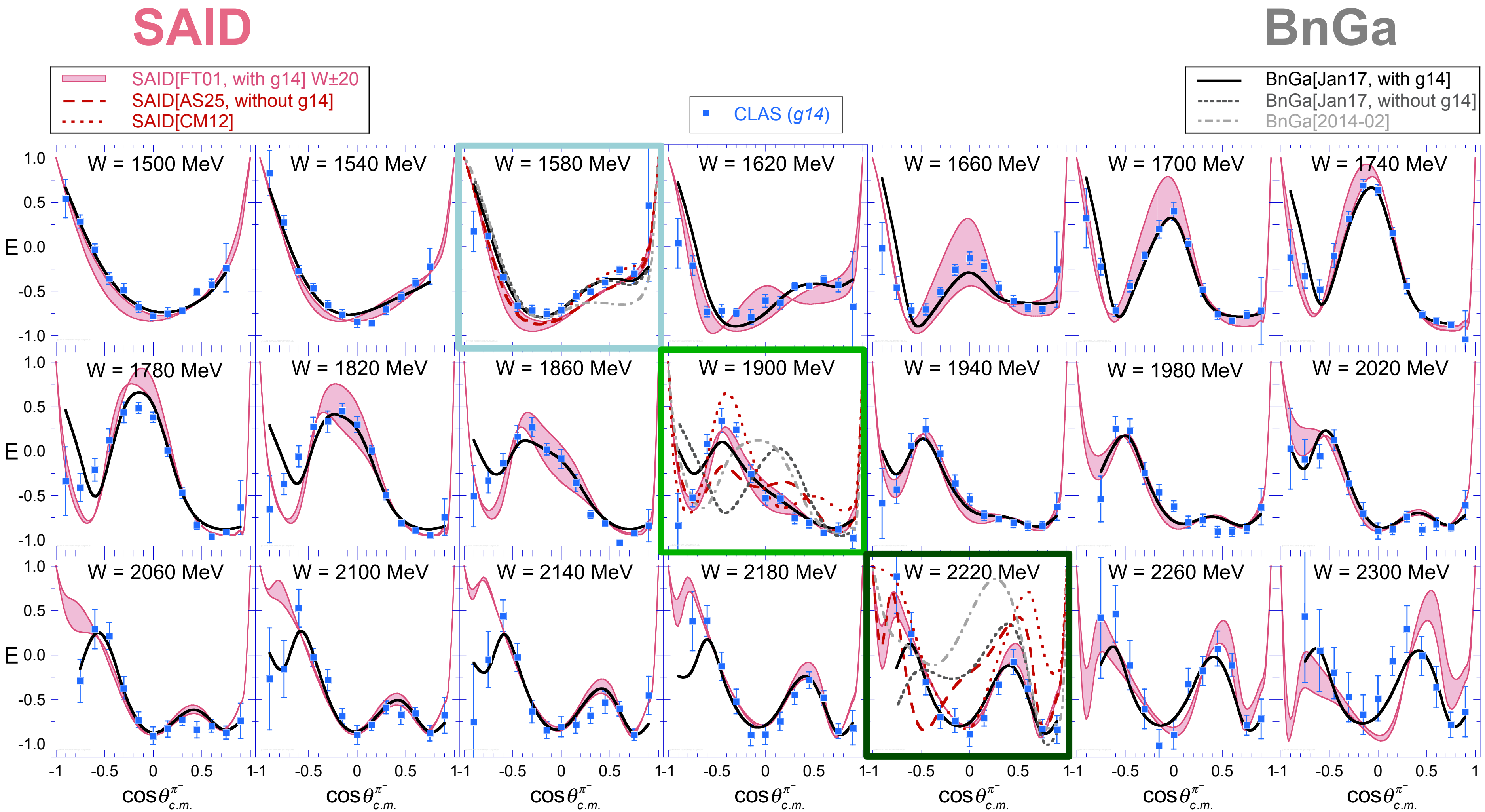

The g14 beam-target "E" asymmetries for $\gamma n \rightarrow \pi^- p$

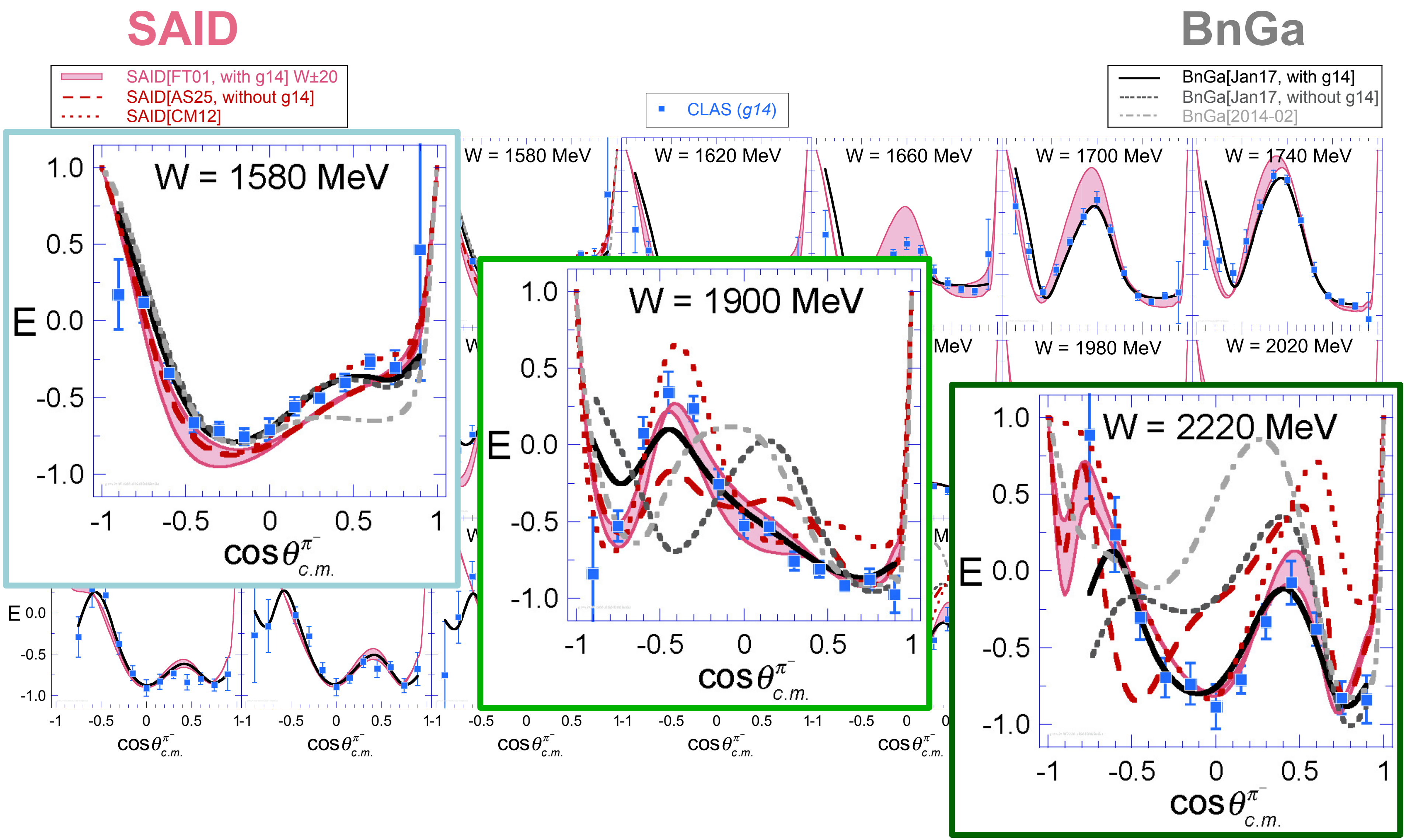

Partial Wave Analyses

$$T_{\alpha\gamma} = \sum_{\sigma} \frac{\bar{K}_{\sigma\gamma}}{\left[1 - c\bar{K}\right]_{\alpha\sigma}}$$

SAID (R. Workman, A. Švarc, I. Strakovsky, …)

- *sequential, unitary fit to all πN scattering and π–photoproduction data*

- fit $\left[1 - c\bar{K}\right]$ to πN ➔ πN and πN ➔ ηN

⇔ determines all poles

- vary K(W) as polynomials in W to fit photo-production

⇔ no *new* resonances

BnGa (E. Klempt, V. Nikonov, A. Sarantsev, …)

- *simultaneous, coupled-channel analysis of πN and γN ➔ πN, ππN, KY*

- fit to SAID amplitudes for πN ➔ πN
- include new resonances as needed to improve fits for γN channels

PWA: phase motion of a resonance

- expectation for an isolated resonance:

- **ideal single isolated resonance** (Breit-Wigner)

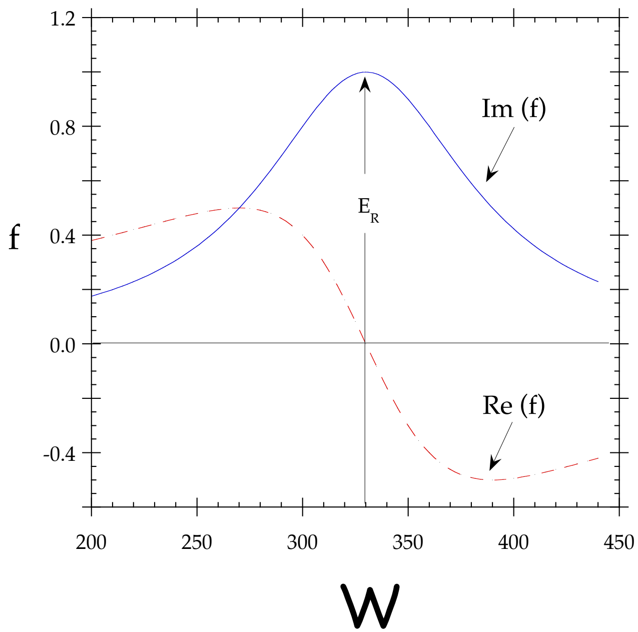

Argand plots:

- **counter-clockwise rotating amplitude**
  - **characteristic resonance behavior**

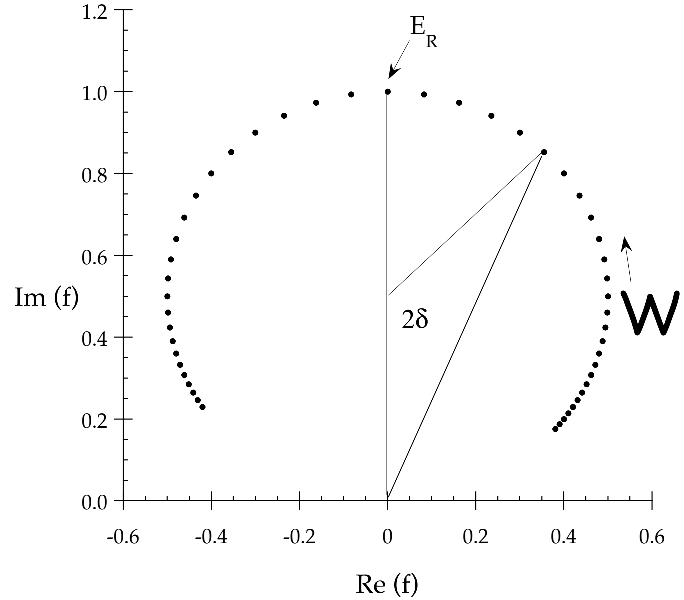

- amplitude decomposed into $(L^{\pi N})_{IJ}(n/p)E/M$ partial waves

PWA: I = 3/2 (Δ^*) partial waves

SAID [AS24; w g14]
SAID [AS25; w/o g14]
SAID [CM12]

eg.

I=3/2, P wave

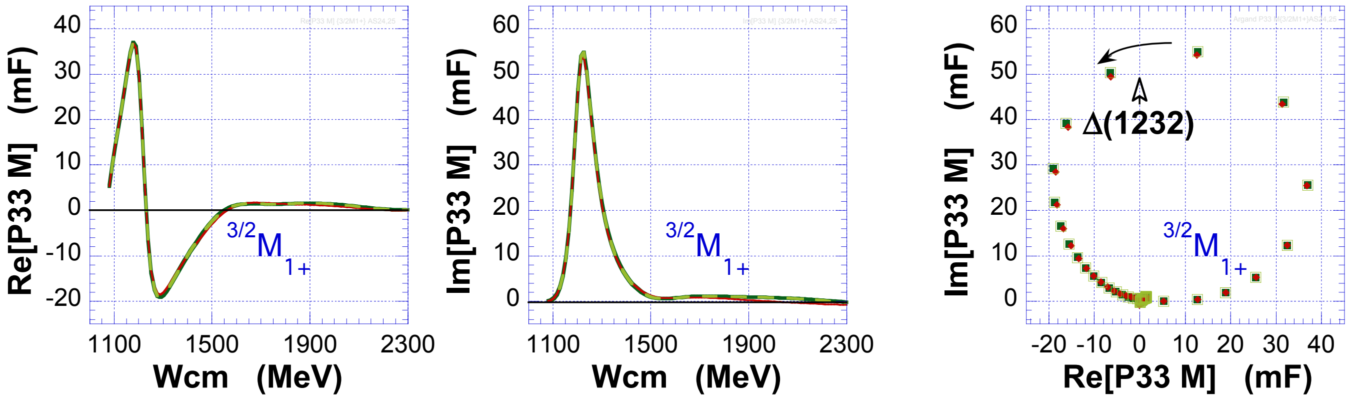

$\Delta(1232)3/2^+$
(PDG ****)

I=3/2, F wave

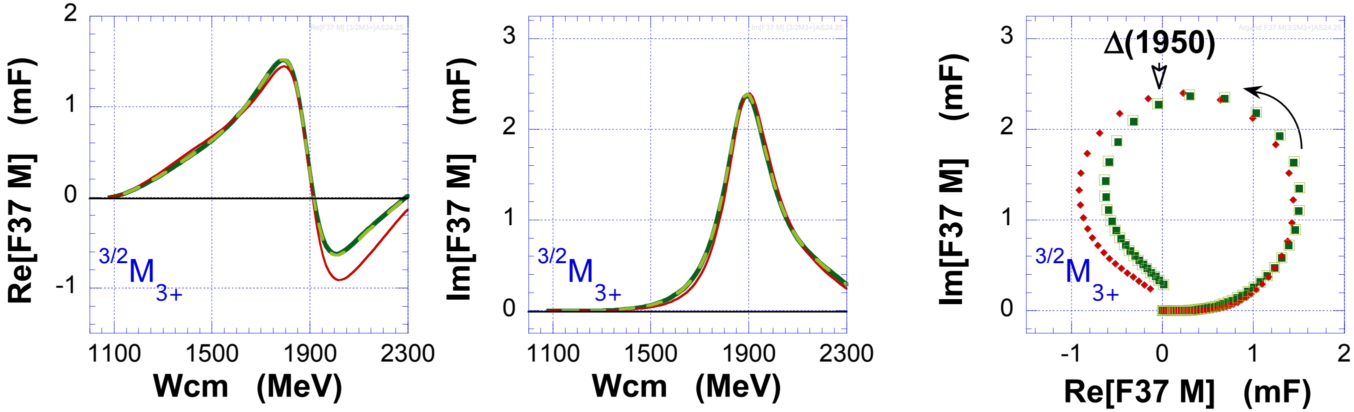

$\Delta(1950)7/2^+$
(PDG ****)

I = 3/2 waves ~ unchanged ⇔ determined by proton data

PWA: I = 1/2 (N^*) P-waves

eg. **SAID P13nM**

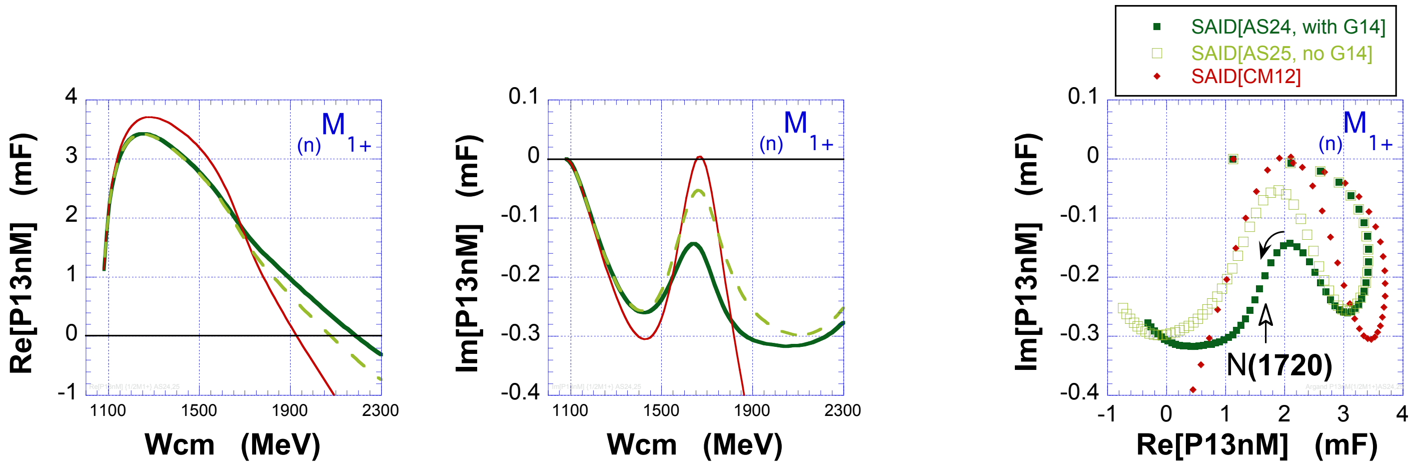

N(1720)3/2⁺ (PDG ****)

BnGa P13nM

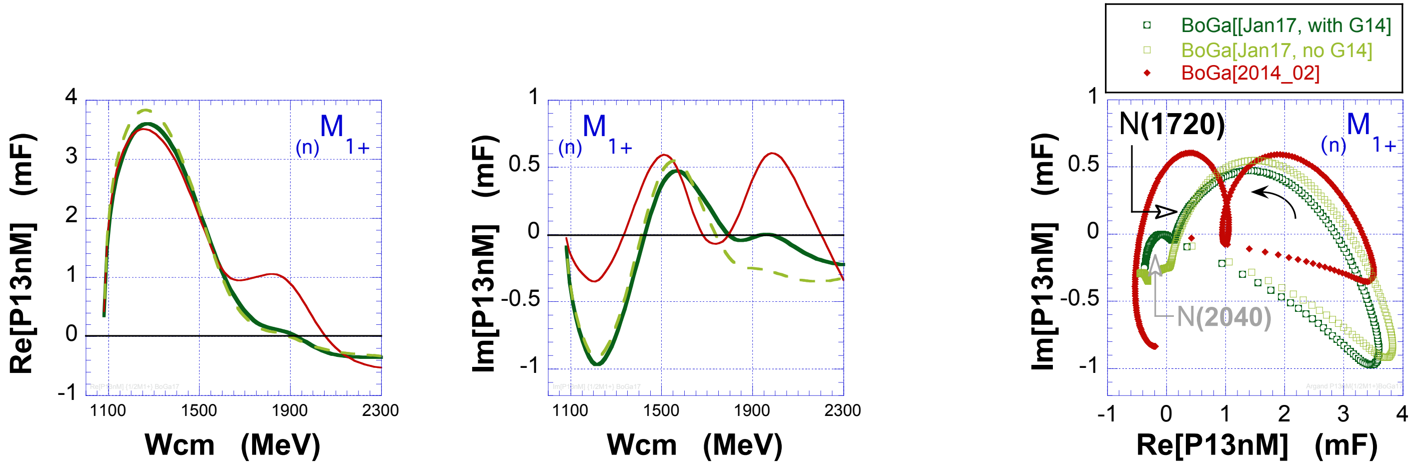

PWA: $I = 1/2$ (N^*) G-waves

eg. **SAID G17nM**

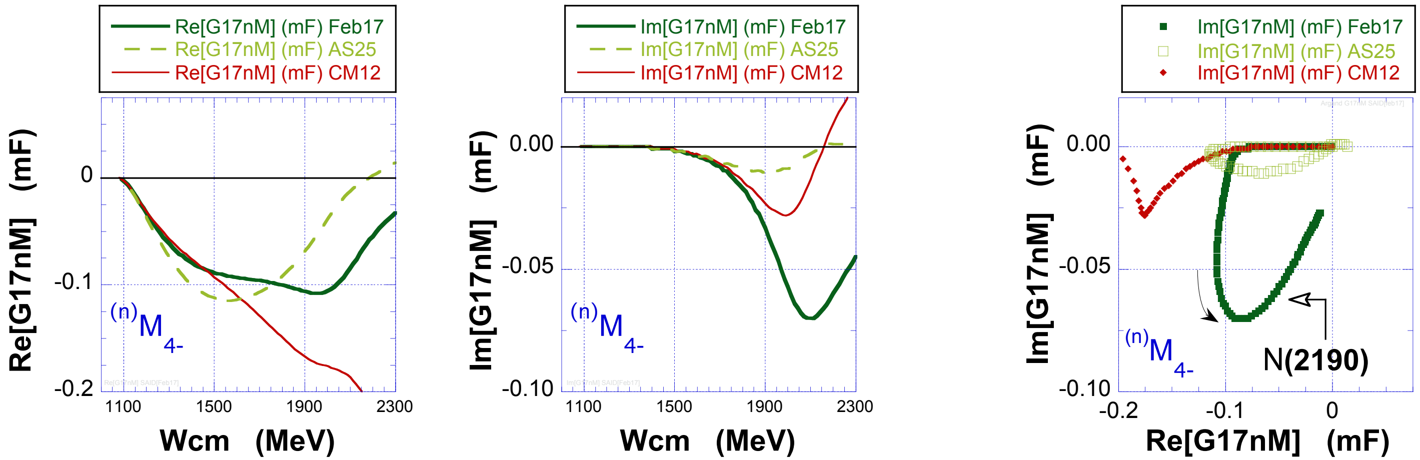

N(2190)7/2⁻
(PDG ****)

BnGa G17nM

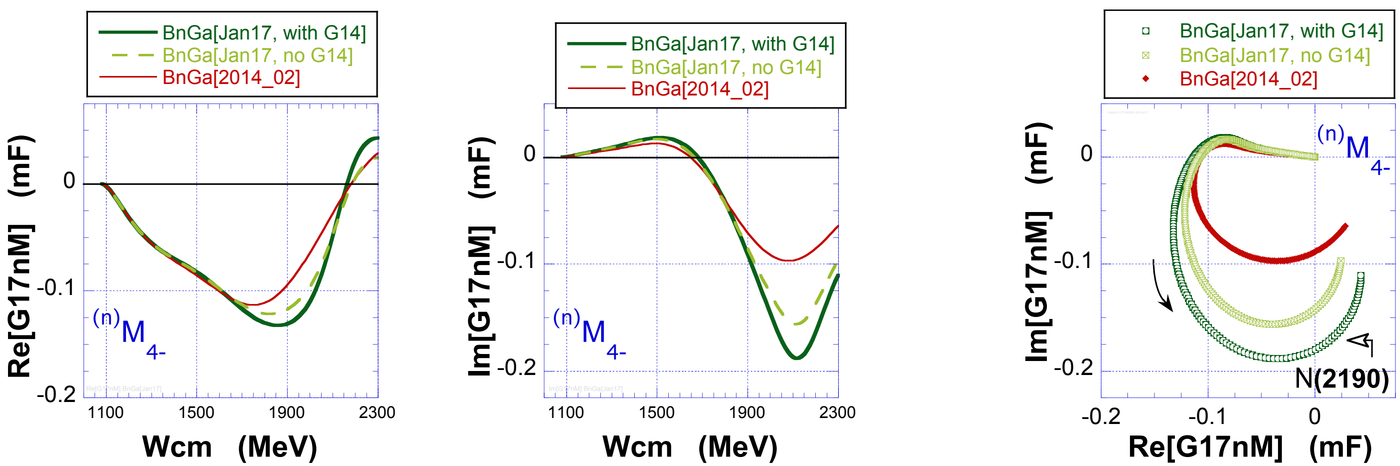

γnN^* couplings ⇔ transverse helicity amplitudes

- $h_\gamma = 1$, $h_N = ½$ ⇔ $A^{1/2}$, $A^{3/2}$
- *residues from analytic continuation to a pole in the complex W plane*
- Breit-Wigner parameterization,

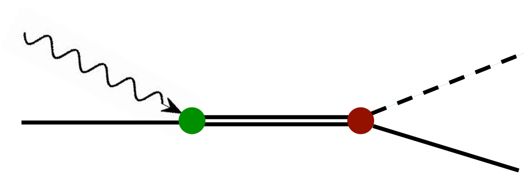

$$T_{\alpha\gamma} = \sum_\sigma \frac{\bar{K}_{\sigma\gamma}}{\left[1 - c\bar{K}\right]_{\alpha\sigma}} \quad \Rightarrow \quad \sum \frac{A^h g_\alpha(s)}{\left[M^2 - s - i\sum c_j g_j^2(s)\right]}$$

revisions to γnN^* couplings

	$A_n^{1/2}$	(10^{-3} GeV$^{-1/2}$)	$A_n^{3/2}$	(10^{-3} GeV$^{-1/2}$)
	g14 PRL	previous	g14 PRL	previous
SAID				
$N(1720)3/2^+$	**-9 ±2**	-21 ±4	**+19 ± 2**	-38 ±7
$N(2190)7/2^-$	**-6 ±9**	---	**-28 ±10**	---
BnGa				
$N(1720)3/2^+$	tbd	-80 ±50	tbd	-140 ±65
$N(2190)7/2^-$	**+30 ±7**	-15 ±12	**-23 ± 8**	-33 ±20

PWA: I = 1/2 (N^*) P-waves

BnGa:

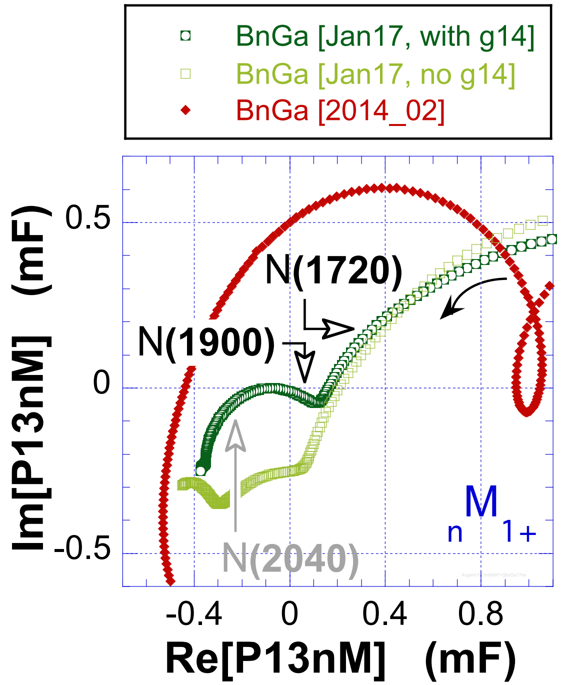

N(1720)3/2⁺ ⬄ PDG ****

N(1900)3/2⁺ ⬄ PDG ****
(but weakly coupled to πN)

N(2040)3/2⁺ ⬄ PDG *

not includes in BnGa PWA
(now under study)

PWA: I = 1/2 (N^*) S-waves

SAID S11nE

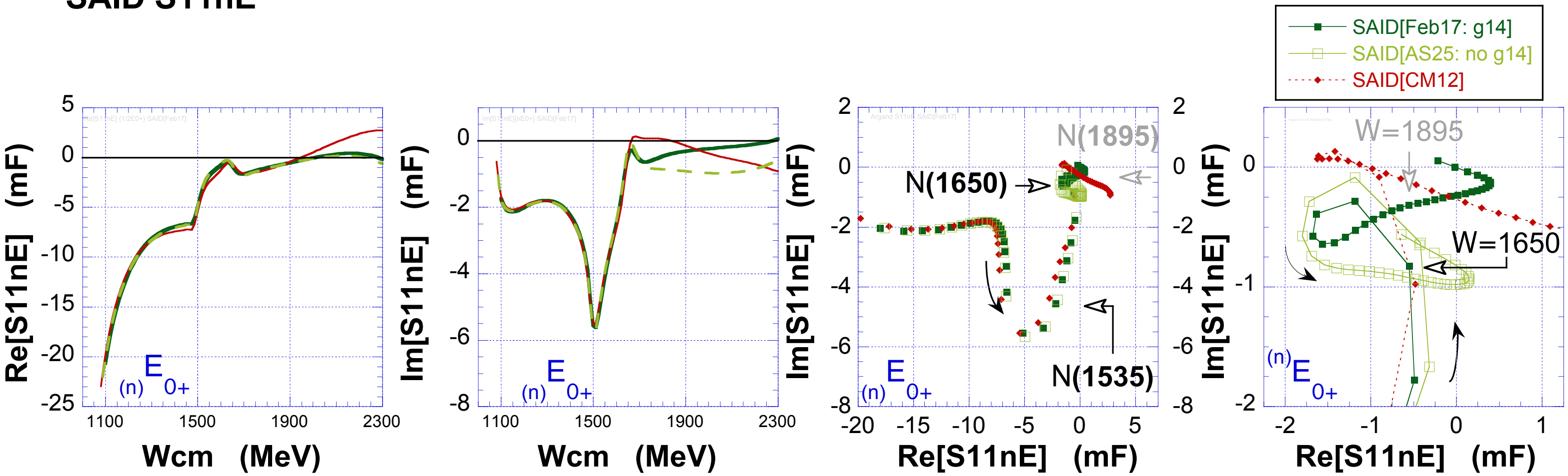

N(1895)1/2⁻ (PDG **)

N(1650)1/2⁻ (PDG ****)

N(1535)1/2⁻ (PDG ****)

BnGa S11nE

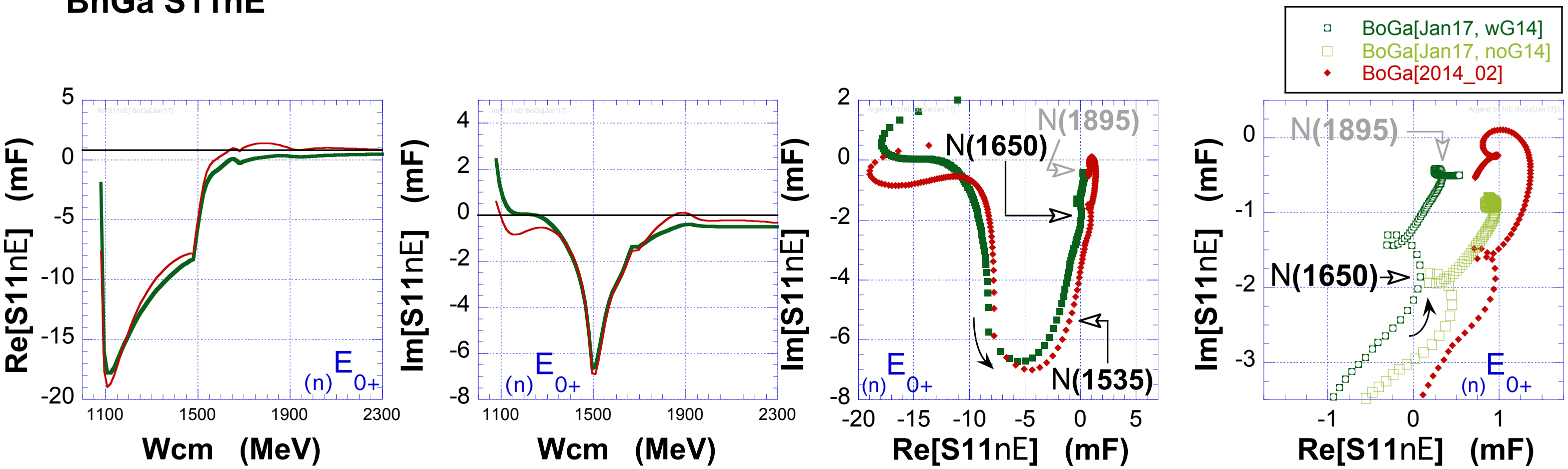

Summary

- *Beam-Target helicity asymmetries (E) for $\gamma n \rightarrow \pi^- p$ just out in PRL*

  - 1st data on this observable and spans the full N energy range*

  - 1st release of g14 data

- *significant addition to the sparse γn data base*

  ⇔ *inclusion in PWA have resulted in significant changes to I = ½ multipoles*

  ⇔ *improved determination of helicity amplitudes ($\gamma n N^*$ couplings) for* N(1720)$3/2^+$ & N(2190)$7/2^-$ *, with SAID and BnGa agreement for $A^{3/2}$*

  ⇔ *potential signals from PDG* and PDG** resonances now under study*

- *next observables in the g14 pipeline:*

  *- beam asymmetry **S** & beam-target asymmetry **G** for $\gamma n \rightarrow \pi^- p$*